JID Open

MicroRNA Expression Patterns Related to Merkel Cell Polyomavirus Infection in Human Merkel Cell Carcinoma

Hong Xie[1,2], Linkiat Lee[1,2], Stefano Caramuta[1,2], Anders Höög[1,3], Nanna Browaldh[4], Viveca Björnhagen[5], Catharina Larsson[1,2] and Weng-Onn Lui[1,2]

Merkel cell carcinoma (MCC) is an aggressive and lethal type of neuroendocrine skin cancer. Mutated Merkel cell polyomavirus (MCV) is commonly found in MCC, and leads to upregulation of the survivin oncogene. However, ~20% of MCC tumors do not have detectable MCV, suggesting alternative etiologies for this tumor type. In this study, our aim was to evaluate microRNA (miRNA) expression profiles and their associations with MCV status and clinical outcomes in MCC. We showed that miRNA expression profiles were distinct between MCV-positive (MCV+) and MCV-negative (MCV−) MCCs and further validated that *miR-203*, *miR-30a-3p*, *miR-769-5p*, *miR-34a*, *miR-30a-5p*, and *miR-375* were significantly different. We also identified a subset of miRNAs associated with tumor metastasis and MCC-specific survival. Functionally, overexpression of *miR-203* was found to inhibit cell growth, induce cell cycle arrest, and regulate survivin expression in MCV− MCC cells, but not in MCV+ MCC cells. Our findings reveal a mechanism of survivin expression regulation in MCC cells, and provide insights into the role of miRNAs in MCC tumorigenesis.

Journal of Investigative Dermatology (2014) **134,** 507–517; doi:10.1038/jid.2013.355; published online 19 September 2013

INTRODUCTION

Merkel cell carcinoma (MCC) is an aggressive type of neuroendocrine skin cancer that affects elderly and immunosuppressed patients. MCC is rare, but its incidence has increased from 0.15 to 0.6 per 100,000 people during 1986 to 2006, and ~1,500 new cases of MCC diagnosed each year in the United States (Bichakjian *et al.*, 2007; Schrama *et al.*, 2012). Although MCC is less common than malignant melanoma, its associated mortality (33%) is approximately double that of melanoma (15%), and ~50% of patients with advanced disease can only survive for 9 months or less (Tai, 2008).

The molecular events involved in MCC development have been partly elucidated. Recently, a new human polyomavirus called Merkel cell polyomavirus (MCV) was identified in MCC tumors (Feng *et al.*, 2008). This virus was detected in ~80% of MCC tumors, where it is clonally integrated into the tumor DNA with tumor-specific T-antigen mutations (Feng *et al.*, 2008; Shuda *et al.*, 2008). The viral T-antigens are also consistently detected in MCC tumors, and they are required for the maintenance of MCV-positive (MCV+) MCC cell growth (Shuda *et al.*, 2008, 2009; Houben *et al.*, 2010). All these features support the important role of MCV in MCC development. However, ~20% of MCC tumors do not have detectable MCV (Feng *et al.*, 2008; Sihto *et al.*, 2009), suggesting alternative unknown etiologies that could in turn be related to the clinical presentation and natural course of this tumor type.

To date, possible differences between MCV+ and MCV-negative (MCV−) MCCs are not well established. Several studies reported an association between MCV status and survival (Sihto *et al.*, 2009; Bhatia *et al.*, 2010; Laude *et al.*, 2010); however, no such association could be confirmed in other studies (Handschel *et al.*, 2010; Schrama *et al.*, 2011). Recently, Arora *et al.* (2012) demonstrated that MCV upregulates survivin in MCCs and this oncogene is a therapeutic target for MCC (Arora *et al.*, 2012). Further investigations are still needed to elucidate the molecular mechanisms of MCC biology for a complete understanding of these tumors and to improve clinical management of this disease.

Here, we investigated the role of microRNAs (miRNAs) in MCC. These small RNAs function by guiding sequence-specific gene silencing, and have been shown to have important regulatory roles in many biological processes (Visone and Croce, 2009). miRNAs are deregulated in many cancer types and specific miRNAs are known to have important roles in

[1]*Department of Oncology-Pathology, Karolinska Institutet, Stockholm, Sweden;* [2]*Cancer Center Karolinska, Karolinska University Hospital, Stockholm, Sweden;* [3]*Department of Clinical Pathology and Cytology, Karolinska University Hospital, Stockholm, Sweden;* [4]*Department of Ear, Nose and Throat, Karolinska University Hospital, Stockholm, Sweden and* [5]*Department of Reconstructive Plastic Surgery, Karolinska University Hospital, Stockholm, Sweden*

Correspondence: Hong Xie or Weng-Onn Lui, Department of Oncology-Pathology, CCK R8:04, Karolinska University Hospital-Solna, 17176 Stockholm, Sweden. E-mail: hong.xie@ki.se or weng-onn.lui@ki.se

Abbreviations: FFPE, formalin-fixed paraffin-embedded; MCC, Merkel cell carcinoma; MCV, Merkel cell polyomavirus; miRNA, microRNA; qRT-PCR, quantitative real-time reverse-transcription–PCR

Received 2 February 2013; revised 4 July 2013; accepted 18 July 2013; accepted article preview online 20 August 2013; published online 19 September 2013

Table 1. Characterization of MCV status in MCC tumors using multiple approaches

	PCR[2]						Immunohistochemistry[3]		
Sample no.[1]	LT3	PS1	LT1	LT3a	VP1	Amplicon(s) confirmed by sequencing	CM2B4	Ab3	MCV status[4]
MCCT_1a	–	–	–	–	–	NA	–	Weak	Neg
MCCT_1b	–	–	–	–	–	NA	–	Weak	Neg
MCCT_2a	–	–	–	–	–	NA	–	Weak	Neg
MCCT_2b	–	–	–	–	–	NA	–	Weak	Neg
MCCT_3a	+	+	+	+	+	ND	–	Strong	Pos
MCCT_3b	+	+	+	+	+	ND	Weak	Strong	Pos
MCCT_4a	+	+	–	+	–	LT3a, PS1	–	Moderate	Pos
MCCT_4b	+	+	–	+	–	LT3, PS1	Weak	Moderate	Pos
MCCT_5a	+	+	+	+	+	ND	Strong	Strong	Pos
MCCT_5b	+	+	–	+	–	LT3, PS1	Moderate	Moderate	Pos
MCCT_6a	+	+	+	+	+	ND	–	Strong	Pos
MCCT_6b	+	+	–	+	–	LT3a, PS1	Weak	Strong	Pos
MCCT_7a	+	+	+	+	+	ND	Weak	Strong	Pos
MCCT_7b	+	+	–	+	–	LT3, PS1	–	Moderate	Pos
MCCT_8	+	+	+	+	+	ND	Strong	Moderate	Pos
MCCT_9	+	+	+	+	+	ND	Moderate	Strong	Pos
MCCT_10	+	+	–	+	–	LT3a, PS1	–	Weak	Pos
MCCT_11	+	+	–	+	–	LT3, PS1	Weak	Moderate	Pos
MCCT_12	–	–	–	–	–	NA	–	–	Neg
MCCT_13	–	–	–	–	–	NA	–	Weak	Neg
MCCT_14	+	+	–	+	–	LT3a	–	Moderate	Pos
MCCT_15	+	–	–	+	–	LT3a, LT3	Weak	Moderate	Pos
MCCT_16	–	–	–	–	–	NA	–	–	Neg
MCCT_17	–	–	–	–	–	NA	–	Weak[5]	Neg
MCCT_18	–	+	–	+	–	LT3a, PS1	–	–	Pos
MCCT_19	+	+	–	+	–	LT3a, PS1	Weak	Moderate	Pos
MCCT_20	+	+	–	+	–	LT3a, PS1	–	Strong	Pos
MCCT_21	–	–	–	–	–	NA	–	Weak	Neg
MCCT_22	+	+	–	+	–	LT3a, PS1	–	Moderate	Pos
MCCT_23	–	–	–	–	–	NA	–	–	Neg
MCCT_24	–	–	–	–	–	NA	–	–	Neg
MCCT_25	+	+	–	+	–	LT3, PS1	Moderate	Strong	Pos
MCCT_26	–	–	–	–	–	NA	–	Weak	Neg

Abbreviations: LT-Ag, large T-antigen; MCV, Merkel cell polyomavirus; NA, not available; ND, not determined; Neg, negative; Pos, positive; –, absent; +, present.

[1]a and b refer to primary and recurrent tumors, respectively, of the same patient.

[2]PCR primers are available in Supplementary Table S1 online.

[3]Detection of MCV LT-Ag expression was performed using CM2B4 (sc-136172; Santa Cruz Biotechnology) and Ab3 (Rodig *et al.*, 2012) antibodies. The staining intensity was scored based on the nuclear immunoreactivity.

[4]MCV positivity was assessed by PCR amplification of the viral genomic DNA with or without moderate to strong expression of LT-Ag using Ab3 antibody.

[5]Moderate staining in perinuclear areas.

tumor development and progression (Iorio and Croce, 2012). Furthermore, miRNAs have been shown to have diagnostic and prognostic values in many cancer types (Calin *et al.*, 2005; Yanaihara *et al.*, 2006; Caramuta *et al.*, 2010). However, the role of miRNAs in MCC has yet to be investigated.

In this study, we characterized the miRNA expression profiles in human MCCs and associated their expressions with MCV status and clinical outcome of the patients. In addition, we determined functional consequences of *miR-203* over-expression in MCC cells.

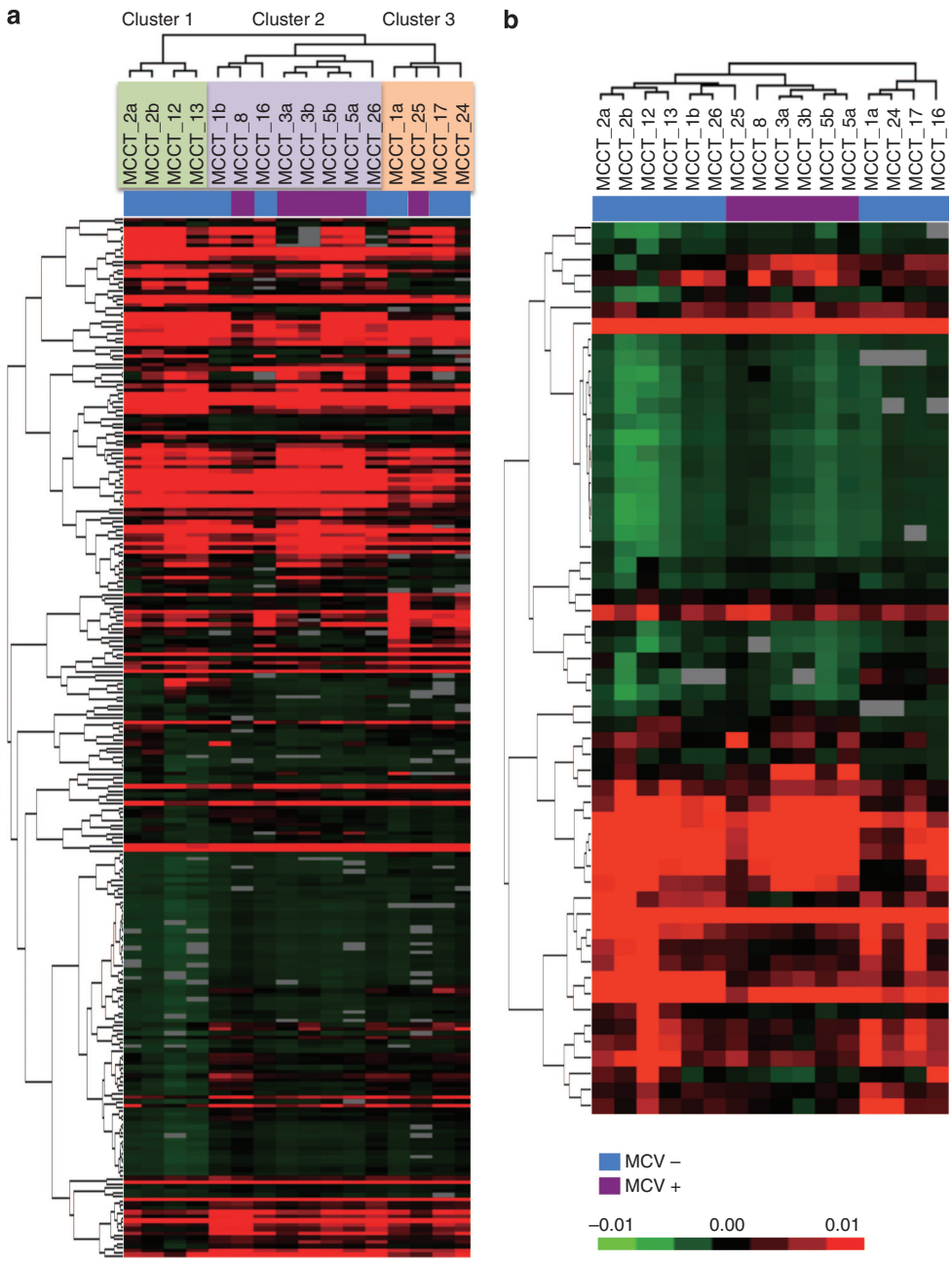

Figure 1. Clustering analysis of microRNA (miRNA) expression in 16 Merkel cell carcinomas (MCCs). (**a**) Samples were clustered based on the 244-filtered miRNAs using unsupervised hierarchical clustering. (**b**) Clustering of the samples was performed using the differentially expressed miRNAs between Merkel cell polyomavirus (MCV) + and MCV − MCCs from significance analysis of microarray (SAM) analysis. The clustering analysis was based on the Spearman rank correlation and complete linkage. Median-centered ratios for each miRNAs are represented. Red and green colors indicate relatively high and low expression, respectively. Missing values are indicated in gray color. The scale bar represents the log10-transformed fold-change values.

RESULTS

Detection of MCV DNA and large T-antigen expression in MCCs

We evaluated MCV status in a series of 33 MCCs using PCR and immunohistochemistry (IHC). For detection of MCV DNA, we amplified viral sequences from tumor DNA using five primer pairs covering different regions of the viral genome (Supplementary Table S1 online). Among the 33 MCCs, we found seven (21.2%) had amplified products for all five primer pairs, 14 (42.4%) showed partial amplifications, and 12 (36.4%) were completely negative for all primer sets (Supplementary Figure S1a online). The PCR products from the cases with partial amplifications were further verified by sequencing (Table 1 and Supplementary Figure S1b online).

For detection of MCV large T-antigen (LT-Ag) expression, we performed IHC using commercially available CM2B4 antibody and the newly raised Ab3 antibody (Rodig *et al.*, 2012). For CM2B4 antibody, 12 of the 33 samples were

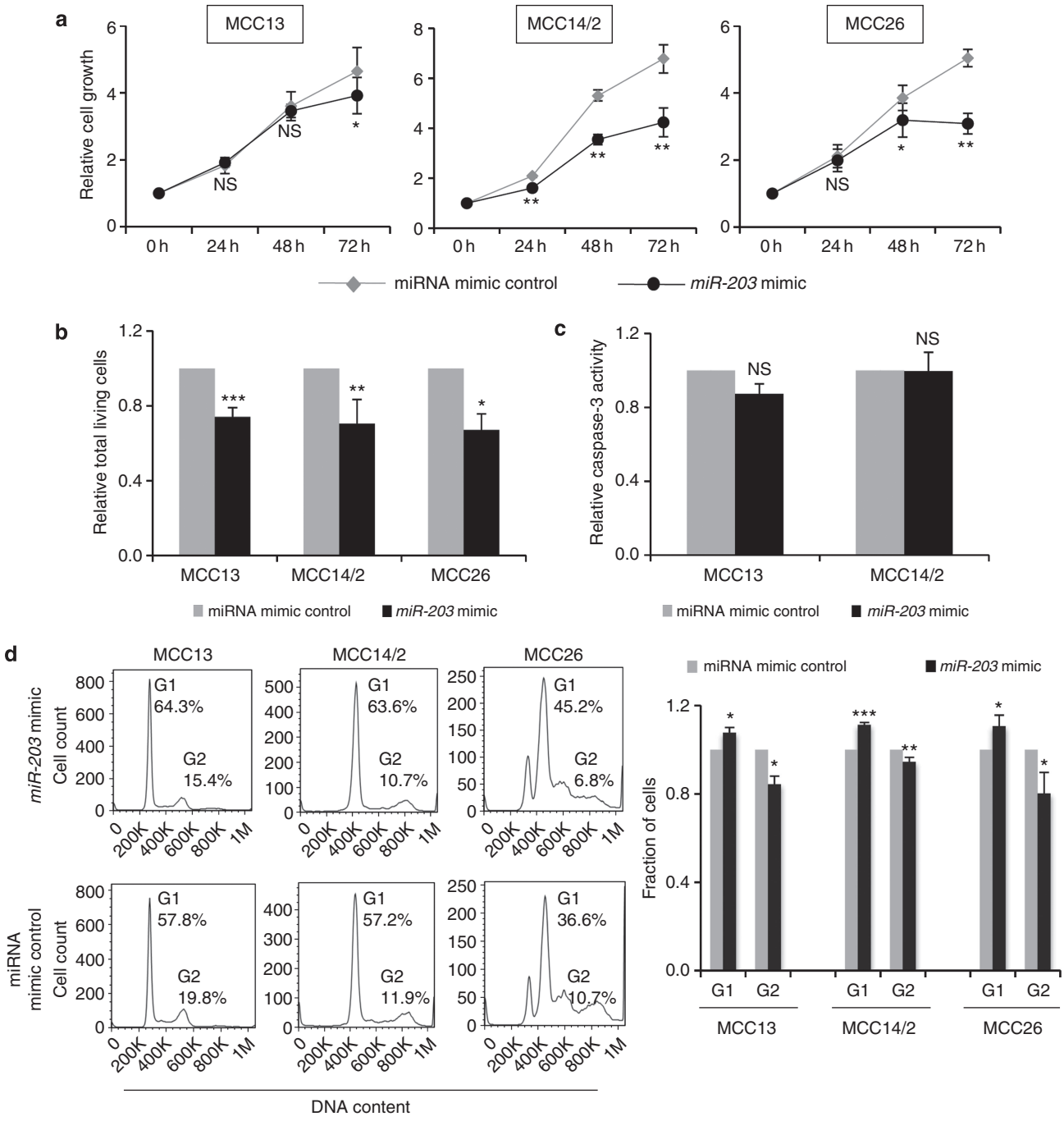

Figure 2. Functional consequences of *miR-203* overexpression in Merkel cell carcinoma (MCC) cells. (**a**) Cell viability was assessed at different time points in MCC cell lines transfected with *miR-203* mimic or negative control using WST-1 assay. (**b**) Trypan blue dye exclusion assay was evaluated at 48 hours after transfection. (**c**) Cell apoptosis was evaluated by caspase-3 colorimetric assay. (**d**) Cell cycle was determined by propidium iodide staining using flow cytometry analysis at 48 hours after transfection. The left panel shows representative histograms of cell cycle analysis from a single experiment, and the right panel shows the cell cycle distributions from three independent experiments. Data represent mean ± SD from at least three independent experiments. *P*-values were calculated using paired Student's *t*-test. $*P<0.05$, $**P<0.01$, $***P<0.001$, NS = not significant.

stained positive in the nuclei of tumor cells; three of which also showed cytoplasmic staining. For Ab3 antibody, the overall staining intensity was higher than the CM2B4 antibody and that stained positively in 28 samples (9 strong, 10 moderate, and 9 weak) and the remaining five samples were negative (Table 1 and Supplementary Figure S2 online).

Four MCCs without MCV LT-Ag immunoreactivity (using both antibodies) were also negative for all amplifications of viral DNA. Eight samples, which were negative for PCR detection of MCV DNA, showed weak immunoreactivity in the nucleus of cancer cells for Ab3 and negative for CM2B4. Tumors classified as MCV+ exhibited positive amplification

of the viral genomic DNA and were with or without moderate to strong expression of MCV LT-Ag using Ab3 antibody. Tumors classified as MCV− revealed no PCR amplification of viral DNA and showed weak or no detectable levels of viral LT-Ag using the Ab3 antibody.

Distinct miRNA expression pattern between MCCs with and without MCV

We asked whether miRNA expression patterns were distinct between MCV+ and MCV− MCCs. We first screened global miRNA profiles in 6 MCV+ and 10 MCV− tumors using a microarray approach. After data normalization and filtering, we performed unsupervised clustering of the 244-filtered miRNAs using Spearman rank correlation and complete linkage. The analysis revealed three distinct clusters (Figure 1a), suggesting distinct biological and/or clinical entities of this tumor type. Interestingly, five of the six MCV+ MCCs were grouped together (cluster 2), whereas the remaining MCV+ tumor was found in cluster 3.

We then applied significance analysis of microarray (SAM) to identify the most significant differentially expressed miRNAs between MCV+ and MCV− MCCs. The analysis identified 36 overexpressed and 20 underexpressed miRNAs in MCV+ tumors (false discovery rate, <30%; Supplementary Table S2 online). On the basis of this classifier, we performed clustering analysis of the same cohort, which resulted in similar but clearer separation between MCV+ and MCV− tumors (Figure 1b). Notably, three out of four matched pairs of MCCs with both primary and recurrent tumors were grouped together, indicating similar miRNA expression profiles between the primary and recurrent tumors.

To validate the microarray results, we evaluated the expression levels of eight miRNAs in an extended series of 32 MCCs (12 MCV− and 20 MCV+) by quantitative real-time reverse-transcription–PCR (qRT–PCR). These miRNAs were selected because of their highest SAM scores and/or their involvement in other tumor types. In concordance with the microarray data, we validated significant overexpression of *miR-30a-3p*, *miR-30a-5p*, *miR-375*, *miR-34a*, and *miR-769-5p* and underexpression of *miR-203* in MCV+ compared with MCV− samples. However, *miR-148a* and *miR-21* were not significantly differentially expressed between MCCs with and without MCV by qRT-PCR (Supplementary Figure S3 online).

miRNAs associated with tumor metastasis and disease-specific survival in MCC

To identify the most significant miRNAs associated with tumor metastasis, we compared miRNA profiles, based on the microarray data, between the primary tumors ($n=9$) and metastases ($n=5$) using SAM analysis. We found only overexpressed miRNAs in MCC metastases with false discovery rate <30%. Ninety-two miRNAs were overexpressed in metastases compared with primary tumors (Supplementary Table S3 online). Notably, four miRNAs (*miR-150*, *miR-630*, *miR-483-5p*, and *miR-142-3p*) had the highest score with a false discovery rate = 0. These miRNAs, together with *miR-146a* (strongly associated with tumor metastasis in other cancer types; Bhaumik *et al.*, 2008; Hurst *et al.*, 2009; Kogo *et al.*, 2011; Hou *et al.*, 2012), were selected for further validation in 17 primary MCCs and nine metastases by qRT-PCR. The results validated overexpression of *miR-150* in the metastases compared with the primary tumors ($P=0.043$; Supplementary Figure S4 online). The other four miRNAs also showed relatively higher expression levels in the metastases compared with the primary tumors; however, the differences were not statistically significant (Supplementary Figure S4 online).

To identify prognostic miRNAs associated with disease-specific survival, we applied SAM survival analysis on the microarray cohort ($n=12$), which resulted in 26 overexpressed and 118 underexpressed miRNAs most correlated with shorter disease-specific survival in MCC (false discovery rate <12%; Supplementary Table S4 online).

Functional consequences of *miR-203* overexpression in MCC cells

Given that *miR-203* has an important role in multiple tumor types (Bo *et al.*, 2011; Li *et al.*, 2011; Noguchi *et al.*, 2012; Jin *et al.*, 2013) and its expression was significantly lower in MCV+ than MCV− MCC tumors, we asked whether *miR-203* has a role in MCC. We ectopically expressed *miR-203* using a miRNA mimic in MCC cell lines and investigated its effect on cell growth, cell cycle, and apoptosis. Using WST-1 and trypan blue exclusion assays, we observed that the cell growth was significantly decreased in the *miR-203* mimic-treated cells compared with its negative control for all three MCV− MCC cell lines (Figure 2a and b). However, we did not observe any significant effect on cell apoptosis upon overexpression of *miR-203*, as evaluated by caspase-3 activity (Figure 2c). We next sought to determine whether *miR-203* regulates cell cycle progression in MCC cells. Indeed, we found that all three MCV− MCC cells transfected with *miR-203* mimic had significantly higher fraction of cells in the G1 phase, whereas the cells in the G2 phase were significantly lower than negative control (Figure 2d). Interestingly, overexpression of *miR-203* in MCV+ WaGa cells had no significant effect on cell proliferation or cell cycle progression (Supplementary Figure S5 online).

miR-203 suppresses survivin expression only in MCV− MCC cells

miR-203 was recently shown to target *survivin* (also known as *BIRC5*) in prostate (Saini *et al.*, 2011b), laryngeal (Bian *et al.*, 2012), and hepatocellular (Wei *et al.*, 2013) cancer cells. Interestingly, *survivin* expression was recently found higher in MCV+ compared with MCV− MCCs (Arora *et al.*, 2012). This prompted us to investigate whether *miR-203* also regulates *survivin* expression in MCCs. We overexpressed *miR-203* in MCC cell lines and assessed its effect on survivin expression at mRNA and protein levels, as determined by qRT-PCR and western blot analysis, respectively. We found that survivin expression was significantly decreased at mRNA and protein levels upon overexpression of *miR-203* in MCV− MCC cells, but not in MCV+ MCC cells (Figure 3a).

MCV T-antigens regulate survivin expression in MCV+ but not in MCV− MCC cells

MCV LT-Ag has been shown to regulate survivin expression in MCV+ MCC cells (Arora *et al.*, 2012). Given that we

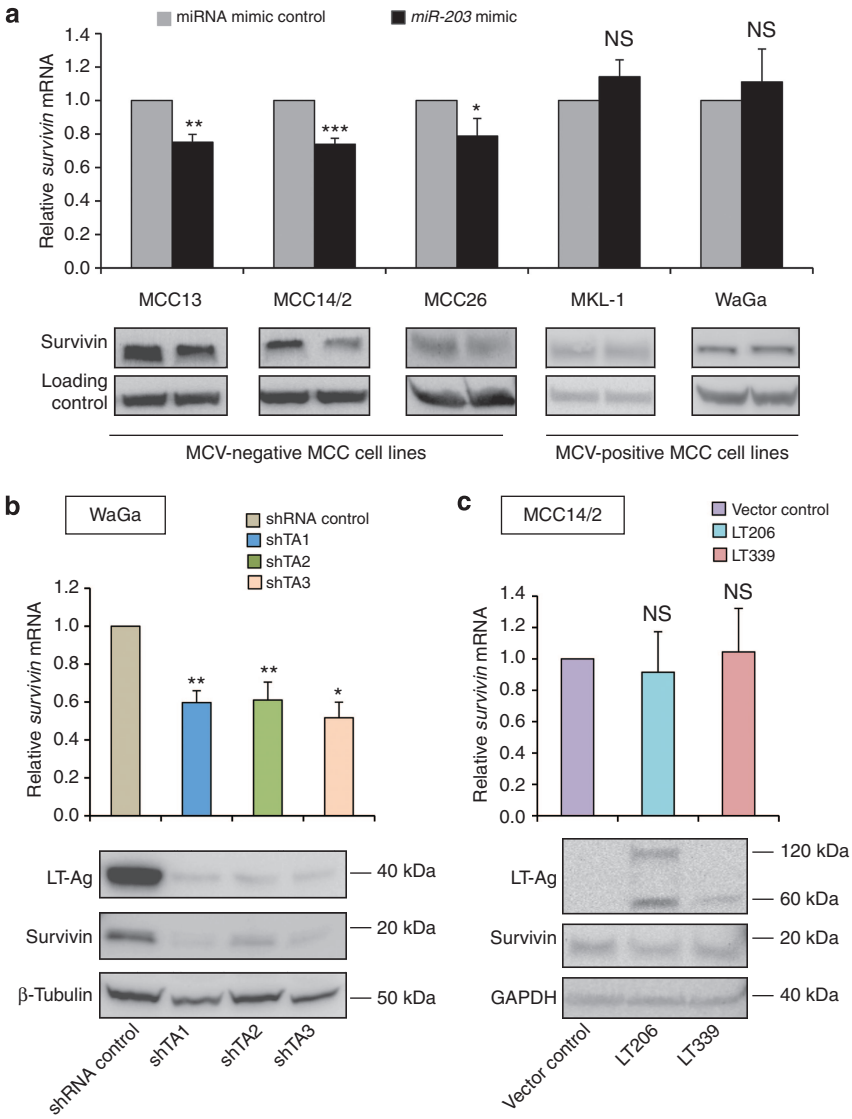

Figure 3. Different regulatory mechanisms of survivin expression in Merkel cell polyomavirus (MCV)+ and MCV− MCC cells. (**a**) MCC cell lines were transfected with *miR-203* mimic or negative control. (**b**) MCV+ WaGa cells were transfected with short hairpin RNAs (shRNAs) against the MCV T-antigens (T-Ag) (shTA1, shTA2, and shTA3) or shRNA control. (**c**) MCV− MCC14/2 cells expressing the wild-type MCV large (L)T-Ag (LT206), truncated MCV LT-Ag (LT339), or empty vector. (**a**–**c**) The upper panels depict quantitative real-time reverse-transcription-PCR (qRT-PCR) analysis of the relative expression of *survivin* mRNA normalized to 18S rRNA, and the lower panels show the representative western blots of LT-Ag, survivin, and loading controls. Data represent mean ± SD from three independent experiments. *$P<0.05$, **$P<0.01$, ***$P<0.001$, NS = not significant (paired Student's *t*-test). GAPDH, glyceraldehyde-3-phosphate dehydrogenase.

observed differences in *miR-203*-mediated survivin expression regulation in MCV+ and MCV− MCC cells, we asked whether MCV LT-Ag also differentially regulates survivin expression between MCC cells with and without the viral factor. We silenced MCV T-Ags using short hairpin RNA (shRNA) constructs targeting the common T-Ag exon 1 sequence in MCV+ WaGa cells and overexpressed wild-type (LT206) or truncated (LT339) MCV LT-Ag in MCV− MCC14/2 cells, and assessed their effects on survivin expressions at both mRNA and protein levels. As shown in Figure 3b, survivin expression was significantly decreased upon silencing of MCV T-Ags. However, we did not observe any significant increase of survivin expression in MCV− MCC14/2 cells expressing either wild-type or truncated MCV LT-Ag (Figure 3c). The results are reproducible in two other MCV− MCC cell lines (MCC13 and MCC26) (data not shown).

DISCUSSION

In this study, we used a genomic approach to characterize miRNA expression profiles of human MCCs. Our results reveal a set of miRNAs associated with MCV status, tumor metastasis, and disease-specific survival in MCC patients.

miRNA expressions in MCC tumors with and without MCV

We show that MCV+ and MCV− tumors are distinct based on miRNA expression profiles. The finding is consistent with the recent study showing distinct mRNA expression profiles

between MCCs with and without MCV (Harms *et al.*, 2013). Our clustering analysis grouped the MCC tumors into three distinct subgroups, suggesting biological or clinical heterogeneity of this tumor type. Notably, we found that the MCV− tumors were grouped into two separate clusters, whereas majority of the MCV+ tumors were grouped together, suggesting distinct molecular mechanisms underlying the pathogenesis of MCV− MCCs. Concordantly, Harms *et al.* (2013) also showed that MCV− MCCs are more heterogeneous than MCV+ tumors based on mRNA expression profiling (Harms *et al.*, 2013).

miR-203 functions as a tumor suppressor in MCC cells

Using SAM analysis, we found a subset of differentially expressed miRNAs between MCV+ and MCV− MCCs. Among them, *miR-203* was found significantly lower in MCV+ tumors, which was further validated in a larger cohort of MCCs by qRT-PCR. *miR-203* is commonly downregulated in human cancers (Chiang *et al.*, 2011; Saini *et al.*, 2011b; Boll *et al.*, 2013; Jin *et al.*, 2013); however, its increased expression has also been observed in breast cancer (Ru *et al.*, 2011), pancreatic cancer (Ikenaga *et al.*, 2010), and ovarian cancer (Iorio *et al.*, 2007). Functionally, *miR-203* has been shown to suppress targets involved in oncogenic processes and pathways in different cancer types (Bo *et al.*, 2011; Li *et al.*, 2011; Saini *et al.*, 2011a; Boll *et al.*, 2013). In this study, we also demonstrate that *miR-203* overexpression inhibits cell growth and induces cell cycle arrest in MCV− MCC cells, suggesting its tumor suppression function in non-viral-associated MCC.

Survivin is one of the direct targets of *miR-203* in several cancer types (Bian *et al.*, 2012; Jin *et al.*, 2013; Wei *et al.*, 2013). We speculated that *survivin* may also be regulated by *miR-203* in MCC, because of its higher expression level in MCV+ than MCV− MCCs and its inverse expression association with *miR-203*. In line with our speculation, we demonstrate that *miR-203* regulates survivin expression only in MCV− MCC cells. However, in MCV+ MCC cells, survivin expression is regulated by MCV LT-Ag oncoprotein. Recently, YM155, a survivin inhibitor, has been shown to inhibit both MCV+ and MCV− MCC cell growth *in vitro* (Arora *et al.*, 2012). Taken together, we propose that survivin is commonly deregulated in MCCs, and it is regulated by MCV LT-Ag in MCV+ MCCs or *miR-203* in MCV− MCCs.

miRNAs associated with tumor metastasis

We identify a subset of miRNAs associated with tumor metastasis in MCC. Among the miRNAs associated with tumor metastasis, increased expression of *miR-150* in MCC metastases is validated by qRT-PCR. This miRNA is highly expressed in hematopoietic cells, and has important roles in hematopoiesis and immune response (Xiao *et al.*, 2007; Zhou *et al.*, 2007; Bezman *et al.*, 2011; Zheng *et al.*, 2012). We noted that seven of the nine tumor metastases included for qRT-PCR analysis are lymph node metastases from MCC primary tumors. The observed higher expression of *miR-150* in the MCC metastases is plausibly due to the high percentage of lymphocytes present in the lymph nodes. Further investigations are warranted to evaluate whether *miR-150* expression is differentially expressed between the lymph node and organ metastases, as well as its functional role in MCC cells.

Among the survival-associated miRNAs, several of them have been associated with tumor progression and survival in other cancer types. For examples, higher expression of *miR-93* has been associated with poor survival in serous ovarian cancer (Nam *et al.*, 2008), and lower expression of *miR-146a* is associated with poor prognosis in gastric cancer (Kogo *et al.*, 2011) and natural killer/T cell lymphoma (Paik *et al.*, 2011). *miR-146a* is known to function as a tumor suppressor in myeloid malignancies (Zhao *et al.*, 2011) and a modulator of the T lymphocyte–mediated immune response (Huffaker *et al.*, 2012). Given that high numbers of intratumoral T lymphocytes in MCC tumors are associated with favorable survival (Iyer *et al.*, 2011; Paulson *et al.*, 2011; Sihto *et al.*, 2012), it is tempting to speculate that *miR-146a* modulates the immune response of the T cells specific for MCV LT-Ag in MCC. Further validation of these prognostic miRNAs in a larger cohort of MCC patients remains to be determined.

Prevalence of MCV infection in MCC tumors

In consistence with previous studies (Feng *et al.*, 2008; Becker *et al.*, 2009; Sastre-Garau *et al.*, 2009; Sihto *et al.*, 2009; Arora *et al.*, 2012; Harms *et al.*, 2013), we found the majority of MCC tumors to be MCV+. However, a subset of MCC tumors were MCV−, which is not in agreement with the recent findings by Rodig *et al.* (2012), who detected MCV LT-Ag expression in almost all MCC tumors using the Ab3 mAb. We used the same antibody concentration ($0.6\,\mu g\,ml^{-1}$) and scoring criteria for evaluating MCV LT-Ag expression in our cohort. However, partly different interpretations of MCV positivity based on Ab3 immunoreactivity were applied. In the study of Rodig *et al.* (2012), weak immunoreactivity (scored as 1+) of Ab3 was interpreted as MCV+. In our study, we could not detect MCV viral genome in those cases with weak immunoreactivity (1+), and therefore scored these cases as MCV−. In Rodig's study, all cases with weak immunoreactivity had very low MCV copy number (<1 copy per cell) that is similar to those cases with lack of immunoreactivity for Ab3, raising a question for the inclusion of 1+ signal as MCV+. Furthermore, previous studies have consistently reported a subset of MCC tumors are MCV− using different approaches (Feng *et al.*, 2008; Becker *et al.*, 2009; Sastre-Garau *et al.*, 2009; Sihto *et al.*, 2009; Arora *et al.*, 2012; Harms *et al.*, 2013). Taken together, we find that the presently available data suggest that a subset of MCCs is MCV−.

In summary, we report miRNA signatures related to MCV infection and clinical outcomes in human MCC. Our findings support that MCV+ and MCV− tumors involved in different genetic pathways, and suggest that MCV− tumors are more heterogeneous than the MCV+ tumors. In addition, we demonstrate the functional role of *miR-203* in MCV− MCC cells, suggesting its role in the pathogenesis of non-viral-associated MCC.

Table 2. Summary of the clinical features of 26 MCC patients in this study

Characteristic (no. of informative)	No. of cases
No. of tumors	33
Gender (n = *26*)	
Male	11
Female	15
Age at diagnosis (n = *26*) *(years)*	
Median = 77 (range 20–91)	
⩽77	14
>77	12
Lesion type (n = *33*)	
Primary	18
Local recurrence	6
Metastasis	9
Primary tumor size (n = *24*) *(cm)*	
Median = 2.4 (range 0.7–15)	
⩽2.4	12
>2.4	12
Primary tumor location (n = *26*)	
Head and neck	15
Arm	5
Other (thigh, gluteal region, groin)	6
Survival (n = *25*) *(months)*	
<12	8
12–60	9
>60	8
Outcome (n = *25*)	
Alive	3
Died of other causes	8
DOD	14
MCV status[1] (n = *33*)	
Positive	21
Negative	12

Abbreviations: DOD, died of disease; LT-Ag, large T-antigen; MCV, Merkel cell polyomavirus.
[1]Detection of MCV genomic DNA combined with LT-Ag immunoreactivity.

MATERIALS AND METHODS

Clinical samples and cell lines

Thirty-three formalin-fixed paraffin-embedded (FFPE) tumor tissues obtained from 26 MCC patients were collected at Karolinska University Hospital or Stockholm South General Hospital (Stockholm, Sweden) from 1986 to 2003. Of these, seven patients had matched pairs of primary and recurrent tumors. The MCC diagnosis was confirmed by histology and IHC at the time of diagnosis. Representative sections from all specimens were histopathologically re-evaluated to confirm high tumor content (>80% tumor cells). The study was approved by the Ethics Committee of Karolinska Institutet and conducted according to the Declaration of Helsinki Principles. The use of archival materials was approved by the Karolinska University Hospital Biobank Unit without written informed consent (BbK-00557). All clinical and histopathological information of the patients are detailed in Supplementary Table S5 online and summarized in Table 2.

Five MCC cell lines were included in this study. Two MCV+ cell lines, MKL-1 and WaGa, were kindly provided by Dr Nancy L. Krett (Northwestern University, Chicago, IL) and Dr Jürgen C. Becker (Medical University of Graz, Graz, Austria), respectively. Three MCV− cell lines, MCC13, MCC14/2, and MCC26, were purchased from CellBank Australia (Westmead, NSW, Australia). All cells were grown in RPMI 1640 medium, supplemented with 10% (MKL-1, WaGa) or 15% (MCC13, MCC14/2, MCC26) fetal bovine serum, and cultured at 37°C with 5% CO_2.

DNA and total RNA extraction

For clinical samples, a 10-μm FFPE section from each specimen was subjected to genomic DNA extraction using QIAamp DNA FFPE Tissue kit (Qiagen, Hildane, Germany). Another 10-μm FFPE section was subjected to total RNA extraction using TRIzol reagent (Invitrogen, Carlsbad, CA) following a previously described method (Ma *et al.*, 2009). For MCC cell lines, genomic DNA was extracted using Qiagen DNeasy Blood and Tissue kit, and total RNA was extracted using mirVana miRNA isolation kit (Applied Biosystems/Ambion, Austin, TX). Plasmid was purified using Qiagen Plasmid Mini Kit. The concentrations of DNA and RNA were measured with a NanoDrop ND-1000 spectrophotometer (NanoDrop Technologies, Wilmington, DE).

MCV DNA detection by PCR and sequencing

The presence of MCV DNA in tumor samples was detected by PCR using previously published primer sets (Feng *et al.*, 2008; Duncavage *et al.*, 2009; Jung *et al.*, 2011); (Supplementary Table S1 online). PCR was performed using 100 ng genomic DNA from tumor samples and cell lines, or 10 ng plasmid DNA. The MKL-1 cell line (Shuda *et al.*, 2008) and the pMCV-R17a (Addgene, Cambridge, MA) plasmid DNA were used as positive controls. The MCC13 cell line (Shuda *et al.*, 2008) and no DNA template were used as negative controls. All PCR amplifications were repeated two times at different time using different DNA preparations. The PCR products from the tumor samples that did not have amplicons for all five primer sets were purified by QIAquick Gel Extraction kit (Qiagen) or ExoSAP-IT (USB Corporation/Affymetrix, Cleveland, OH), and sequenced at the KIGene core facility.

miRNA microarray experimentation and analyses

miRNA expression profiling was performed using Agilent's human miRNA microarray (miRBase release 10.1; Agilent, Santa Clara, CA), as described previously (Caramuta *et al.*, 2010). In brief, 200 ng of total RNA was labeled with Cy3 and then hybridized onto the arrays for 20 hours at 55 °C. Slides were scanned using Agilent microarray scanner (Agilent, Santa Clara, CA). The images were processed with Feature Extraction Software 10.7.3.1 (Agilent). Intensity values were normalized and median centered using Cluster 3.0. Only normalized miRNAs with <20% missing values across the samples were used for clustering and statistical analyses. Hierarchical clustering was performed based on complete linkage with the Spearman rank

correlation using Cluster 3.0 and visualized with Treeview version 1.60 (de Hoon *et al.*, 2004). SAM (http://www-stat.stanford.edu/~tibs/SAM/) was used to determine the association of miRNAs with MCV status, tumor metastasis, and disease-specific survival. Microarray data are available at NCBI Gene Expression Omnibus (GEO accession number GSE43699).

qRT-PCR

Expression of mature miRNAs and mRNA was quantified by qRT-PCR using the Applied Biosystems 7900HT or StepOne Plus Real-time PCR systems. For mature miRNAs, cDNA was synthesized from 50 ng (for FFPE samples) or 100 ng (for cell lines) total RNAs using TaqMan MicroRNA Reverse Transcription Kit (Applied Biosystems). Predesigned TaqMan MicroRNA Assays for *miR-30a-3p* (ID 000416), *miR-30a-5p* (ID000417), *miR-34a* (ID000426), *miR-148a* (ID000470), *miR-769-5p* (ID001998), *miR-21* (ID000397), *miR-375* (ID000564), *miR-203* (ID00507), *miR-483-5p* (ID002338), *miR-150* (ID000473), *miR-142-3p* (ID000464), *miR-146a* (ID000468), and *miR-630* (ID001563) were purchased from Applied Biosystems. *RNU6B* (ID001093) was used for normalization of miRNA expression. For mRNA quantification, cDNA was synthesized from 100 ng total RNAs using High Capacity cDNA Reverse Transcription kit (Applied Biosystems). qRT-PCR was performed for *BIRC5* (Hs04194329_s1; Applied Biosystems) and normalized against *18S* ribosomal RNA (Hs99999901_s1; Applied Biosystems). All reactions were performed in triplicate and relative expression levels were reported as $2^{-\Delta CT}$.

Construction of expression and shRNA vectors

Wild-type (LT206, plasmid 28190) and truncated (LT339, plasmid 28193) MCV LT-Ag expression vectors (Shuda *et al.*, 2008) were purchased from Addgene. As a negative control, we used an empty vector, which was constructed by deleting the insert from the LT339 plasmid by digestion with *Xba*I and *Nhe*I (New England Biolabs, Ipswich, MA).

We cloned three shRNA vectors targeting the common exon 1 of MCV T-antigens between *Bgl*II and *Kpn*I sites of plasmid pcDNA3-U6M2 (Taft *et al.*, 2011). The targeting sequences of the shRNAs are described in Supplementary Figure S6 online. All constructs were confirmed by sequencing at KIGene core facility.

Transfection

For small RNA transfection, MCC13, MCC14/2, and MCC26 cells were transfected with 10 nM of *miR-203* mimic (Applied Biosystem) or miRNA mimic Negative Control no. 1 (Applied Biosystem) using Lipofectamine RNAiMAX Reagent (Invitrogen) following the reverse transfection method as described in the manufacturer's protocol. WaGa cells were transfected with 10 pmol per 1×10^6 cells of *miR-203* mimic or negative control using Lipofectamine RNAiMAX Reagent (Invitrogen). MKL-1 cells were transfected with 20 pmol per 1×10^6 cells of *miR-203* mimic or negative control by Nucleofector Kit V (Amaxa/Lonza, Basel, Switzerland) using program A-24. For MCV LT-Ag expression vector transfection, MCC14/2 cells were transfected with LT206, LT339, or empty vector (2 μg per well in a 6-well plate) using Lipofectamine 2000 Reagent (Invitrogen). For shRNA vector transfection, 2 μg shRNA vector (pcDNA3-U6M2, shTA1, shTA2, and shTA3) were transfected into 1×10^6 WaGa cells by Nucleofector Kit V and program D-24.

Western blot analysis

At 48 or 72 hours after transfection, cells were collected and lysed for immunoblot analysis as described previously (Xie *et al.*, 2012). Survivin antibody (1:1,000; no. 2808; Cell Signaling Technology, Danvers, MA) was used to determine survivin expression, CM2B4 (1:200, sc-136172; Santa Cruz Biotechnology, Santa Cruz, CA) was used to determine MCV LT-Ag expression, glyceraldehyde-3-phosphate dehydrogenase (1:10,000, sc-47724; Santa Cruz Biotechnology) or β-tubulin (1:1,000; no. 2128; Cell Signaling Technology) was used for normalization. Signals were detected by LAS-1000 Image Analyzer (Fujifilm, Tokyo, Japan), and protein expressions were quantified using Image Gauge version 4.0 (Fujifilm).

Immunohistochemistry

CM2B4 and Ab3 (kindly provided by Dr James A. DeCaprio, Dana-Farber Cancer Institute, Boston, MA) antibodies were used for IHC to determine MCV LT-Ag expression in clinical samples. Four-μm tissue sections were deparaffinized, rehydrated, and blocked for endogenous peroxidase with 3% hydrogen peroxide. Antigen retrieval was performed at ~99°C in citrate buffer (pH 6.0; for CM2B4) or Tris-EDTA buffer (pH 9.0; for Ab3). The antibodies (CM2B4, 1:100; Ab3, 0.6 μg ml^{-1}) were diluted with Dako REAL antibody diluent (Dako Denmark A/S, Glostrup, Denmark), applied on the tissues, and incubated overnight at 4 °C. Anti-mouse/rabbit horseradish peroxidase–conjugated antibody was applied on tissues for 40 minutes at room temperature before developing with Dako REAL EnVision Detection System (Dako), and counterstained with Mayer's hematoxylin. The immunoreactivity was examined under a light microscope, and scored based on nuclear immunoreactivity by a pathologist (A Höög).

Cell growth analysis

For WST-1 assay, 8.0×10^3 cells per well (MCC13 and MCC14/2), 4.0×10^3 cells per well (MCC26), or 4.0×10^4 cells per well (WaGa) in 100 μl culture medium were seeded into 96-well plate. At different time points (0, 24, 48, 72, or 96 hours after transfection), 10 μl of WST-1 reagent was added and incubated for 3 hours at 37 °C. Absorbance was determined at 450 nm (measurement) and 650 nm (reference) using a VERSAmax microplate reader (Molecular Devices, Sunnyvale, CA). Each experimental group consisted of eight replicates for each time point. All experiments were performed at least three times independently. Cell growth rate was evaluated by subtracting the background absorbance individually and normalized to 0-hour time point.

For trypan blue exclusion assays, cells were collected at 48 or 72 hours after transfection, stained with 0.4% trypan blue stain (Invitrogen), and analyzed using a TC10 automated cell counter (Bio-Rad, Hercules, CA). The total live cells in *miR-203* mimic–transfected cells were normalized to the miRNA mimic–negative control.

Cell apoptosis assay

Apoptosis assay was performed using caspase-3 colorimetric assay kit (BioVision, Mountain View, CA), as described previously (Xie *et al.*, 2012). In brief, 5×10^5 cells were transfected and harvested after 48 hours of transfection, and lyzed in 50 μl of chilled cell lysis buffer for 10 minutes. A total of 50 μl protein lysate (4 mg ml^{-1}) was mixed with 50 μl of 2 × Reaction Buffer and 5 μl of 4 mM caspase-3 substrate, and incubated for 2 hours at 37 °C. Detection of the caspase-3

cleavage products was measured at 405 nm using a VERSAmax microplate reader (Molecular Devices). Relative caspase-3 activity was determined by the absorbance values of the samples compared with the respective negative controls. All experiments were replicated three times independently.

Cell cycle analysis

At 48 or 72 hours after transfection, 1×10^6 cells were washed with phosphate-buffered saline and fixed in cold 50% ethanol for 1 hour. After washing with phosphate-buffered saline and treating with RNase A ($0.2\,mg\,ml^{-1}$) for 1 hour at 37 °C, the cells were stained with propidium iodide ($0.04\,mg\,ml^{-1}$). Cell cycle analysis was performed using flow cytometry (Cytomics FC 500; Beckman Coulter, Brea, CA) and FlowJo software version 7.6.2 (Tree Star, Ashland, OR). All experiments were performed independently in triplicate.

Statistical analyses

Statistica 7.0 (StatSoft, Tulsa, OK) or Microsoft Office Excel 2007 was used for statistical calculations, unless otherwise stated. The comparison between miRNA expressions in different groups was conducted using unpaired Student's *t*-test. Paired Student's *t*-test was performed to analyze transfection experiments. Patients who are alive or died of MCC-unrelated reasons were considered as censored. All the analyses were two-tailed and *P*-values <0.05 were regarded as significant.

CONFLICT OF INTEREST

The authors state no conflict of interest.

ACKNOWLEDGMENTS

This work was supported by the Swedish Research Council (523-2009-3517; 521-2010-3518), the Åke Olsson's Foundation for Haematological Research, the Swedish Cancer Foundation, the Åke Wiberg's Foundation, the Cancer Research Funds of Radiumhemmet, the Axel and Signe Lagerman's Donation Foundation, Karolinska Institutet, and Stockholm County Council. HX is a recipient of the Karolinska Institutet PhD support program. We thank Susanne Agartz, Lisa Viberg, and Lisa Ånfalk from Biobank of Karolinska University Hospital for all clinical samples, Dr Nancy L Krett (Northwestern University) for providing MKL-1 cell line, Dr Jürgen C Becker (Medical University of Graz) for providing WaGa cell line, Dr James A DeCaprio (Dana-Farber Cancer Institute) for providing Ab3 antibody, Dr Yu Ming (Karolinska Institutet) for providing glyceraldehyde-3-phosphate dehydrogenase primers, Per Johansson (Karolinska Institutet) for the plasmid pCDNA3-U6M2, and Zhangsen Huang and Linjing Zhu (Karolinska Institutet) for technical support of flow cytometry. We also thank the staff at the KIGene core facility for sequencing service, and all members of Medical Genetics research group for helpful discussions and suggestions.

SUPPLEMENTARY MATERIAL

Supplementary material is linked to the online version of the paper at http://www.nature.com/jid

REFERENCES

Arora R, Shuda M, Guastafierro A *et al.* (2012) Survivin is a therapeutic target in Merkel cell carcinoma. *Sci Transl Med* 4:133–56

Becker JC, Houben R, Ugurel S *et al.* (2009) MC polyomavirus is frequently present in Merkel cell carcinoma of European patients. *J Invest Dermatol* 129:248–50

Bezman NA, Chakraborty T, Bender T *et al.* (2011) miR-150 regulates the development of NK and iNKT cells. *J Exp Med* 208:2717–31

Bhatia K, Goedert JJ, Modali R *et al.* (2010) Merkel cell carcinoma subgroups by Merkel cell polyomavirus DNA relative abundance and oncogene expression. *Int J Cancer* 126:2240–6

Bhaumik D, Scott GK, Schokrpur S *et al.* (2008) Expression of microRNA-146 suppresses NF-kappaB activity with reduction of metastatic potential in breast cancer cells. *Oncogene* 27:5643–7

Bian K, Fan J, Zhang X *et al.* (2012) MicroRNA-203 leads to G1 phase cell cycle arrest in laryngeal carcinoma cells by directly targeting survivin. *FEBS Lett* 586:804–9

Bichakjian CK, Lowe L, Lao CD *et al.* (2007) Merkel cell carcinoma: critical review with guidelines for multidisciplinary management. *Cancer* 110:1–12

Bo J, Yang G, Huo K *et al.* (2011) microRNA-203 suppresses bladder cancer development by repressing bcl-w expression. *FEBS J* 278:786–92

Boll K, Reiche K, Kasack K *et al.* (2013) MiR-130a, miR-203 and miR-205 jointly repress key oncogenic pathways and are downregulated in prostate carcinoma. *Oncogene* 32:277–85

Calin GA, Ferracin M, Cimmino A *et al.* (2005) A microRNA signature associated with prognosis and progression in chronic lymphocytic leukemia. *N Engl J Med* 353:1793–801

Caramuta S, Egyhazi S, Rodolfo M *et al.* (2010) MicroRNA expression profiles associated with mutational status and survival in malignant melanoma. *J Invest Dermatol* 130:2062–70

Chiang Y, Song Y, Wang Z *et al.* (2011) Aberrant expression of miR-203 and its clinical significance in gastric and colorectal cancers. *J Gastrointest Surg* 15:63–70

de Hoon MJ, Imoto S, Nolan J *et al.* (2004) Open source clustering software. *Bioinformatics* 20:1453–4

Duncavage EJ, Zehnbauer BA, Pfeifer JD (2009) Prevalence of Merkel cell polyomavirus in Merkel cell carcinoma. *Mod Pathol* 22:516–21

Feng H, Shuda M, Chang Y *et al.* (2008) Clonal integration of a polyomavirus in human Merkel cell carcinoma. *Science* 319:1096–100

Handschel J, Muller D, Depprich RA *et al.* (2010) The new polyomavirus (MCPyV) does not affect the clinical course in MCCs. *Int J Oral Maxillofac Surg* 39:1086–90

Harms PW, Patel RM, Verhaegen ME *et al.* (2013) Distinct gene expression profiles of viral- and nonviral-associated merkel cell carcinoma revealed by transcriptome analysis. *J Invest Dermatol* 133:936–45

Hou Z, Yin H, Chen C *et al.* (2012) MicroRNA-146a targets the L1 cell adhesion molecule and suppresses the metastatic potential of gastric cancer. *Mol Med Report* 6:501–6

Houben R, Shuda M, Weinkam R *et al.* (2010) Merkel cell polyomavirus-infected Merkel cell carcinoma cells require expression of viral T antigens. *J Virol* 84:7064–72

Huffaker TB, Hu R, Runtsch MC *et al.* (2012) Epistasis between microRNAs 155 and 146a during T cell-mediated antitumor immunity. *Cell Rep* 2:1697–709

Hurst DR, Edmonds MD, Scott GK *et al.* (2009) Breast cancer metastasis suppressor 1 up-regulates miR-146, which suppresses breast cancer metastasis. *Cancer Res* 69:1279–83

Ikenaga N, Ohuchida K, Mizumoto K *et al.* (2010) MicroRNA-203 expression as a new prognostic marker of pancreatic adenocarcinoma. *Ann Surg Oncol* 17:3120–8

Iorio MV, Croce CM (2012) MicroRNA involvement in human cancer. *Carcinogenesis* 33:1126–33

Iorio MV, Visone R, Di Leva G *et al.* (2007) MicroRNA signatures in human ovarian cancer. *Cancer Res* 67:8699–707

Iyer JG, Afanasiev OK, McClurkan C *et al.* (2011) Merkel cell polyomavirus-specific CD8(+) and CD4(+) T-cell responses identified in Merkel cell carcinomas and blood. *Clin Cancer Res* 17:6671–80

Jin J, Deng J, Wang F *et al.* (2013) The expression and function of microRNA-203 in lung cancer. *Tumour Biol* 34:349–57

Jung HS, Choi YL, Choi JS *et al.* (2011) Detection of Merkel cell polyomavirus in Merkel cell carcinomas and small cell carcinomas by PCR and immunohistochemistry. *Histol Histopathol* 26:1231–41

Kogo R, Mimori K, Tanaka F *et al.* (2011) Clinical significance of miR-146a in gastric cancer cases. *Clin Cancer Res* 17:4277–84

Laude HC, Jonchere B, Maubec E *et al.* (2010) Distinct Merkel cell polyomavirus molecular features in tumour and non tumour specimens from patients with merkel cell carcinoma. *PLoS Pathogen* 6:e1001076

Li J, Chen Y, Zhao J *et al.* (2011) miR-203 reverses chemoresistance in p53-mutated colon cancer cells through downregulation of Akt2 expression. *Cancer Lett* 304:52–9

Ma Z, Lui WO, Fire A *et al.* (2009) Profiling and discovery of novel miRNAs from formalin-fixed, paraffin-embedded melanoma and nodal specimens. *J Mol Diagn* 11:420–9

Nam EJ, Yoon HJ, Kim SW *et al.* (2008) MicroRNA expression profiles in serous ovarian carcinoma. *Clin Cancer Res* 14:2690–5

Noguchi S, Mori T, Otsuka Y *et al.* (2012) Anti-oncogenic microRNA-203 induces senescence by targeting E2F3 protein in human melanoma cells. *J Biol Chem* 287:11769–77

Paik JH, Jang JY, Jeon YK *et al.* (2011) MicroRNA-146a downregulates NFkappaB activity via targeting TRAF6 and functions as a tumor suppressor having strong prognostic implications in NK/T cell lymphoma. *Clin Cancer Res* 17:4761–71

Paulson KG, Iyer JG, Tegeder AR *et al.* (2011) Transcriptome-wide studies of merkel cell carcinoma and validation of intratumoral CD8+ lymphocyte invasion as an independent predictor of survival. *J Clin Oncol* 29:1539–46

Rodig SJ, Cheng J, Wardzala J *et al.* (2012) Improved detection suggests all Merkel cell carcinomas harbor Merkel polyomavirus. *J Clin Invest* 122:4645–53

Ru P, Steele R, Hsueh EC *et al.* (2011) Anti-miR-203 upregulates SOCS3 expression in breast cancer cells and enhances cisplatin chemosensitivity. *Genes Cancer* 2:720–7

Saini S, Arora S, Majid S *et al.* (2011a) Curcumin modulates microRNA-203-mediated regulation of the Src-Akt axis in bladder cancer. *Cancer Prev Res (Philadelphia)* 4:1698–709

Saini S, Majid S, Yamamura S *et al.* (2011b) Regulatory role of miR-203 in prostate cancer progression and metastasis. *Clin Cancer Res* 17:5287–98

Sastre-Garau X, Peter M, Avril MF *et al.* (2009) Merkel cell carcinoma of the skin: pathological and molecular evidence for a causative role of MCV in oncogenesis. *J Pathol* 218:48–56

Schrama D, Peitsch WK, Zapatka M *et al.* (2011) Merkel cell polyomavirus status is not associated with clinical course of Merkel cell carcinoma. *J Invest Dermatol* 131:1631–8

Schrama D, Ugurel S, Becker JC (2012) Merkel cell carcinoma: recent insights and new treatment options. *Curr Opin Oncol* 24:141–9

Shuda M, Arora R, Kwun HJ *et al.* (2009) Human Merkel cell polyomavirus infection I. MCV T antigen expression in Merkel cell carcinoma, lymphoid tissues and lymphoid tumors. *Int J Cancer* 125:1243–9

Shuda M, Feng H, Kwun HJ *et al.* (2008) T antigen mutations are a human tumor-specific signature for Merkel cell polyomavirus. *Proc Natl Acad Sci USA* 105:16272–7

Sihto H, Bohling T, Kavola H *et al.* (2012) Tumor infiltrating immune cells and outcome of Merkel cell carcinoma: a population-based study. *Clin Cancer Res* 18:2872–81

Sihto H, Kukko H, Koljonen V *et al.* (2009) Clinical factors associated with Merkel cell polyomavirus infection in Merkel cell carcinoma. *J Natl Cancer Inst* 101:938–45

Taft RJ, Hawkins PG, Mattick JS *et al.* (2011) The relationship between transcription initiation RNAs and CCCTC-binding factor (CTCF) localization. *Epigenet Chromatin* 4:13

Tai P (2008) Merkel cell cancer: update on biology and treatment. *Curr Opin Oncol* 20:196–200

Visone R, Croce CM (2009) MiRNAs and cancer. *Am J Pathol* 174:1131–8

Wei W, Wanjun L, Hui S *et al.* (2013) miR-203 inhibits proliferation of HCC cells by targeting survivin. *Cell Biochem Funct* 31:82–5

Xiao C, Calado DP, Galler G *et al.* (2007) MiR-150 controls B cell differentiation by targeting the transcription factor c-Myb. *Cell* 131:146–59

Xie H, Zhao Y, Caramuta S *et al.* (2012) miR-205 expression promotes cell proliferation and migration of human cervical cancer cells. *PLoS One* 7:e46990

Yanaihara N, Caplen N, Bowman E *et al.* (2006) Unique microRNA molecular profiles in lung cancer diagnosis and prognosis. *Cancer Cell* 9:189–98

Zhao JL, Rao DS, Boldin MP *et al.* (2011) NF-kappaB dysregulation in microRNA-146a-deficient mice drives the development of myeloid malignancies. *Proc Natl Acad Sci USA* 108:9184–9

Zheng Q, Zhou L, Mi QS (2012) MicroRNA miR-150 is involved in Valpha14 invariant NKT cell development and function. *J Immunol* 188:2118–26

Zhou B, Wang S, Mayr C *et al.* (2007) miR-150, a microRNA expressed in mature B and T cells, blocks early B cell development when expressed prematurely. *Proc Natl Acad Sci USA* 104:7080–5